Available online at www.sciencedirect.com

ScienceDirect

Procedia Manufacturing 7 (2016) 39 – 45

Procedia MANUFACTURING

International Conference on Sustainable Materials Processing and Manufacturing, SMPM 2017, 23-25 January 2017, Kruger National Park

Characteristics of laser *In-situ* alloyed titanium aluminides coatings

Monnamme Tlotleng*, Bathusile Masina[a], Sisa Pityana[a,b]

[a]*Laser Enabled Manufacturing Group NLC, Council for Scientific and Industrial Research, Pretoria, 0001, South Africa*
[d]*Department of Chemical and Metallurgical Engineering, Tshwane University of Technology, Pretoria, 0001, South Africa*

Abstract

The use of titanium aluminides as high temperature materials in the aerospace and automobile industries is becoming a reality since their early research and development in 1955. Their mechanical properties at elevated temperatures make them attractive in spite of their poor ductility at room temperature. The progress on their production using powder metallurgy processes seem to be significantly positive; at least on microstructure tailoring and mechanical properties. This research work sought to study the *in-situ* alloying of the elemental Ti and Al using laser metal deposition (LMD) process. The effects of laser power on the microstructure evolution, composition and micro-hardness were evaluated on the as-produced TiAl coatings. The results indicated that lamellar microstructures formed at 1.0, 1.3 and 1.5 kW laser powers while at 2.0 kW a refined dendritic structure was observed. The phase composition by XRD concluded the presence of $TiAl_3$, TiAl, Ti_3Al_5, and the oxide phases of Ti and Al. Generally, the Ti_3Al_5 phase is indicative of high temperature process during TiAl processing while $TiAl_3$ is known as a twinning phase to TiAl. The average $HV_{0.3}$ values for 1.0, 1.3, 1.5 and 2.0 kW coatings were $327_{0.3}$, $281_{0.3}$, $333_{0.3}$ and $367_{0.3}$, respectively. These hardness values are indicative of the presence of $TiAl/TiAl_3$.

Peer-review under responsibility of the organizing committee of SMPM 2017

Keywords: Hardness, Heat-input, Laser-power, Microstructures, Titanium aluminides (TiAls) and X-ray diffraction (XRD).

* Correspond author
Email address: MTlotleng@csir.co.za

Peer-review under responsibility of the organizing committee of SMPM 2017
doi:10.1016/j.promfg.2016.12.013

1. Introduction

Titanium aluminides (TiAl) are primarily intermetallic materials that can be used as thermal barrier coatings in surface science and engineering or as near net shaped components for aircrafts and automotive vehicles [1]. According to the Ti-Al phase diagram, thermodynamically, elemental Al and Ti can react to form different intermetallics, some of which are not necessary as engineering structures or surface coatings due to their unstable characteristics in their environment of use. The gamma (γ)-TiAl and Ti_3Al phases are of engineering interest [2, 3] hence they are being researched. The γ-TiAl phase have been used successfully in manufacturing miniature turbo gas chargers for vehicles where they have aided in the reduction of fuel consumption and increase in performance due to their light-weight property [4]. Concurrently, there are others who seek to use stable TiAl phase materials as surface barrier coatings for high temperature engineering applications where they can self-oxidise and act as barrier coatings [5-12].

The microstructure of the resulting TiAl can be achieved by allowing the diffusion of Al into Ti matrix, between 22 – 48 atomic %, while oxidation can be promoted by adding stabilisers to rutile and/or alumina powders as opposed to having self-oxidation occurring during processing [11,13]. The experimental designs on the promotion of ductility and self-oxidising characteristics of the TiAl structures have led to the production of pre-alloyed ternary system powders which are currently being used as feedstock during the manufacturing of TiAl components. There is published scientific research on the use of Electron Beam Melting [14], Laser Engineering Net Shaping [15] and Laser Metal Deposition processes [16, 17] in the synthesis of defects free TiAl coupons and structures using pre-alloyed powders. From the reviewed literature, Löber et al [18] and Gussone et al [19] used selective laser melting (SLM) processes to manufacture TiAl and studied their microstructure. Qu and Wang [20] and Qu et al [21] used LMD to manufacture TiAl from the pre-alloyed powders. The LMD results concluded a dual phase, fully lamellar microstructure.

Lasers by definition offers controlled operation and, rapid heating and cooling while the convection forces present in the melt pool can promote rates of diffusion where co-fed powders can mix. The aspects of manufacturing TiAl alloys using laser materials processes including the LMD technique and the Laser-Engineering Net-Shape (LENS) system are being investigated by the Laser Enabled Manufacturing (LEM) Group at the National Laser Centre CSIR, Pretoria, South Africa. The preliminary results reported in this work are on the effects of laser power during the *in-situ* alloying of Ti and Al into TiAl aluminides coatings. The resulting microstructure, composition and the hardness of the produced coatings are presented and discussed.

2. Experimental methods

2.1. Materials

Commercially available pure titanium and aluminium powders were used for deposition in this study. Both powders had a particle size distribution of 45-90 μm and were supplied by TLS, Technik GmbH & Co. The powders were used as received. Ti-6Al-4V base plates of 70 x 70 x 5 mm^3 dimensions were used as substrates. Before deposition the base plates were sand-blasted and cleaned with acetone. The sand blasting step promotes adhesion of the coating to the substrate during processing.

2.2. Laser metal deposition

A 3kW IPG continuous fibre laser system was used in this study. This laser is continuously cooled with a chiller. A 1.5 bar GTV powder feeder system, that uses two hoppers, was used to contain and control the powders during processing. A bulk compressed Argon gas supply tank, with high volume control regulators, was used as both the powder carrier and shielding gas. A copper coaxial 3-way nozzle was used to inject the powder plume into the melt pool that was already created on the substrate. The laser beam angle and stand-off distance of 13° and 12 mm were used, respectively. The process parameters used were: laser power (1-2 kW), beam spot size (4 mm), and shielding

gas flowrate (10l/min), powder carrier gas flowrate (2l/min) and scanning speed (2.5 m/min). The powder carrier gas was set to provide *in-situ* alloying of 80 % titanium with 20 % aluminium.

2.3. Sample preparation and characterisation

The LMD TiAl prepared coatings were brushed with a wire brush post processing and prepared for metallographic observations. Keller's reagent was used for etching at 2-3 minutes. The microstructures and elemental analyses were conducted using Joel JSM-6010PLUS/LA scanning electron microscope (SEM) that used Intouch Scope software for analyses. Panalytical XPert Pro PW 3040/60 X-ray diffraction with Cu Kα monochromater radiation source was used for phase analyses while Matsuzawa Seiko Vickers model MHT-1 was used for the micro-hardness analyses conducted at indent-load of 300 g and 10 seconds dwelling time.

3. Results and Discussions

3.1. Microstructural Analyses

Optical images in Fig. 1 illustrate the overall TiAl coatings fabricated by laser depositing Ti and Al powders on the Ti-6Al-4V substrate when the laser power was increased from above (a) 1.0 kW, (b) 1.3 kW, (c) 1.5 kW and 2.0 kW. The thickness of the produced coatings averaged at 1.185±0.135 mm; which was considerably similar. The optical analyses present the cross sectional defects such as macro-cracks and pores when the laser power was increased from 1.0-2.0 kW. The analyses are consistent with the general laser-materials interaction theory. The theory estimates that during laser-materials processing the heat inputs are directly proportional to the laser power when the laser beam scanning speed is kept constant. The laser beam scanning speed relates directly to the material-laser beam residence time. The residence time controls the degree of heating and melting the substrate and the deposited materials.

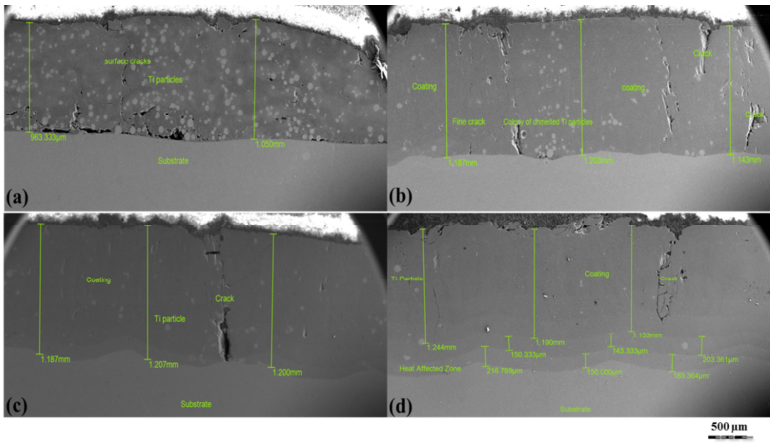

Fig. 1. The as product TiAl coatings (a) 1.0 kW, (b) 1.3 kW, 1.5 kW and (d) 2.0 kW.

It is evident from Fig. 1 (a) that the coating does not entirely adhere to the substrate. This might be because the laser power was low therefore led to poor melt pool temperature being achieved. It is also evident that the coating was porous and there was poor diffusion of the aluminium into the titanium particles that could not be melted at 1.0 kW. The colony of unmelted particles of Ti-Al at 1.0 kW can be deduced from fig. 1(a). The observed unmelted particles seemed to have decreased with the increase in the laser power. In Fig. 1 (b), improvement on the coating adhesion and porosity were observed with higher concentrations of macro-cracks being visible. Observations on Figs. 1 (c and d) led to an understanding that material dilution of about ±150 µm into the substrate was present and

created a stronger bond. The dilution effects, due to increased heat inputs as a result of increased laser power (2.0 kW), is evident in Fig. 1 (d).

The microstructures of the coatings in Fig. 2 indicate that TiAl lamellar structures were formed during laser processing from 1.0-2.0 kW. The coatings from the 2.0 kW laser power, however led to the formation of the dendrite rich coating. The observed lamellar were mixed (bilateral) at 1.0 kW, became refined, homogenous and unilateral at 1.3 kW and then coarse at 1.5 kW. The formed coatings reached the third stage of reaction.

$$Ti_x + Al_y \rightarrow \alpha\text{-}Ti_3Al \rightarrow TiAl_2 \rightarrow TiAl_3$$

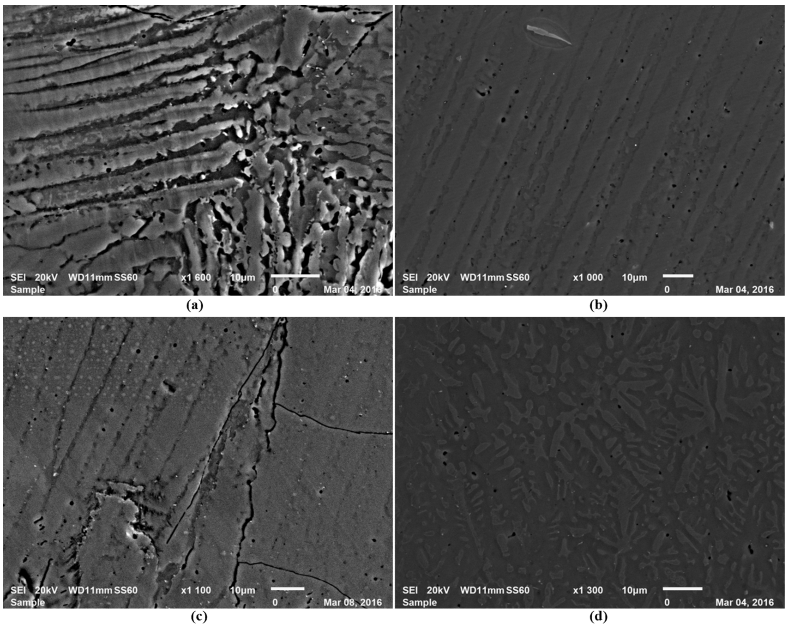

Fig. 2. SEM Microstructure analyses of the TiAl 2.0 kW.

The SEM microstructures of the coatings in Fig. 2 indicate that the coatings were lamellar at 1.0 to 1.5 kW. The lamellar structures were disoriented at 1.0 kW, became ordered and refined at 1.3 kW, and finally coarse at 1.3 kW. This showed that a further increase in the laser power lead to the structural ordering and refinement, but there is a threshold which this study can be assumed to be at 1.3 kW. A further increase of laser power to 2.0 kW led to the formation of the primary dendritic structures. These observations then conclude that 1.3 kW is more suitable to refine the lamellar structure of the resulting TiAl structures that form during direct laser metal *in-situ* alloying process.

3.2. Composition

The compositions of the laser *in-situ* produced TiAl coatings were obtained by means of analysing the diffraction peaks as presented in Fig. 3. The assignment of the diffraction peaks was performed according to the X-Pert Pro Ti – Al database using appropriate PDF files: Al (04-012-3403), Ti (00-005-0682), TiO_2 (00-015-0875), Al_2O_3 (00-004-0877), $AlTiO_2$ (00-052-1557), $TiAl_3$ (04-018-4873), Ti_3Al_5 (00-042-0810), $TiAl_2$ (00-042-1136). The overall observation from the peaks informs that there is a positive slight shift towards the higher 2θ with the increase in laser power. There is a peak convolution that occurred at the peak positions in the range 42-48, 65-85 and 75-85°. Deconvolution is observed at peaks position of 20-21° and 65-66°. The deconvolution led to doublets being formed while convolution led to the broadening of the peaks which resulted in a slight drop in the intensities. The peak

position of single phase Ti and Al are missing which are indicative of the formation of new phases resulting due to the reaction that occurred during melting of these elemental powders.

What is most interesting about the presented peaks, at different laser powers, is that the diffraction peaks seem to be getting refined with the increase in laser power which could suggest that an increase in heat input led to good melting and diffusion of Al into Ti matrix thereby resulting in a more uniform and stable crystalline material or a homogenous coating being achieved. More importantly, the absence of single phase index peaks of the Ti or Al in the presented diffraction peaks indicates clearly that mixtures between the two elements were achieved. The diffraction peaks deduces that the composition became more stable while self-oxidising with the increase in the laser power. The aluminium oxide layer is prominent at 38.79° at 1.0 kW power.

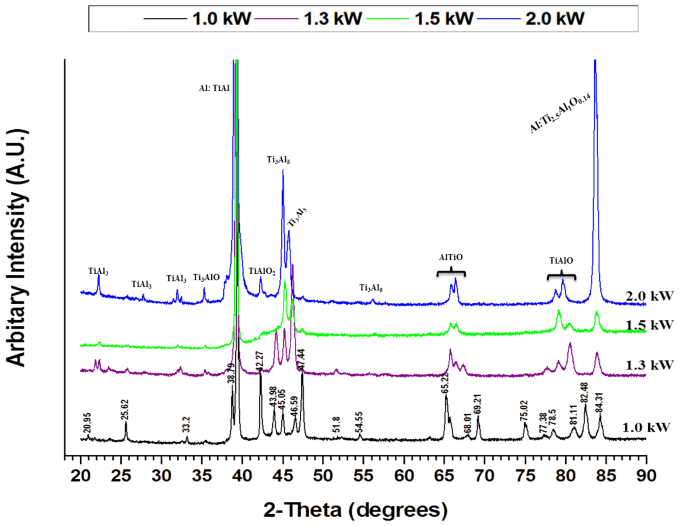

Fig. 3. The X-ray diffraction peak of the as produced coatings.

3.3. Hardness Measurement

The micro-hardness measurements produced by this study are reported in Table 1. The hardness values reported in Table 1 showed an insignificant variation in the average hardness. In addition, this study observed that the hardness values may differ at the top and bottom of the coatings. In general, the hardness results suggested that the lamellar hardness trend was as follow: coarse>disorder>>thin, ordered lamellar while the observed dendrites were hardest. Ma et al [22] reported that thin lamellar have maximum hardness when compared to the thick lamellar and inter-dendritic γ-phase. Shishkovsky et al [16] reported an overall hardness range of 130-800 HV for TiAl laser produced coatings. They attributed this HV range to the intermetallic phase locations that are present in the coatings. The presented average hardness range in this study falls within the cited range.

Table 1: Summary of the hardness values.

Laser power (kW)	Top ($HV_{0.3}$)	Middle ($HV_{0.3}$)	Average ($HV_{0.3}$)
1.0	366	288	320
1.3	280	283	305

1.5	334	332	350
2.0	327	372	374

Table 1 concluded that the hardness increased by about ±24 HV with the laser power, except for the 1.3 kW produced coating which had the lowest average hardness values of 305 HV.

In this study we expect the heat input to increase with the laser power setting since the scanning speed was kept constant throughout. The average Vickers hardness values for TiAl is 300 HV [27] or 350±5 HV and 285±5 HV for TiAl and Ti3Al [28], respectively. Murr et al (2010) reported the average hardness value of 418.1 HV for TiAl materials produced with EBM. Guo et al (2007), using laser cladding process, observed a wavy hardness profile. The hardness increased with the aluminium content in the formed TiAl coatings. The coating with 80Ti/20Al was least hard, by extrapolation, with the average hardness of about 630 HV at the top and 460 HV in the middle. Our hardness results are similar to those reported by Guo et al.

4. Conclusion

In summary, the results presented in this paper are consistent with literature; a contradiction is only observed with the overall hardness on the lamellar formed TiAl structures. The microstructures, XRD and hardness values support that TiAl and Ti_3Al are congruent at high temperature processes and the XRD indexes show explicitly that Ti_3Al5 will be the only phase detected as it has already been reviewed. The direct laser metal deposition process was evaluated in the fabrication of the TiAl coatings using elemental Ti and Al powers that were injected simultaneous from different hoppers and processed at different laser powers while keeping the laser scanning speed constant. The results concluded that:

- It is possible to produce TiAl coating from elemental Ti and Al using laser metal *in-situ* alloying method;
- The produced microstructures showed lamellar at laser power between 1.0-1.5 kW and a dendritic-rich microstructure of TiAl with 2.0 kW;
- The phase analyses revealed that the coatings comprised of $TiAl_3$ and Ti_3Al_5. Both phases are stable and are associated with high temperature processes;
- The hardness measurements revealed that the coatings are indeed of the TiAl/$TiAl_3$ making.

Acknowledgements

This work was funded through the CSIR PG grant on Additive Manufacturing and 3D Printing. The authors would also like to thank the NLC team for assistance and their continued support.

References

[1] E. Illeková, J. Gachon, A. Rogachev, H. Grigoryan, J.C. Schuster, A. Nosyrev, P. Tsygankov, Thermochimica Acta. 469 (2008) 77-85.
[2] N. Kosova, V. Schkov, I. Kurzina, A. Pichugina, A. Vladimirov, L. Kazantseva, A. Sachkova, IOP Conf. Series: Mater. Sci. Eng. 112 (2016) 1-5.
[3] E. Hamzah, M. Kanniah, M. Harun, Jurnal. Teknologi. 43 (2005) 113-124.
[4] M. Yamaguchi, H. Inui, K. Ito, Acta Materialia. 48 (2000) 307-322.
[5] L.M. Hsiung, T.G. Nieh, Mater. Sci. Eng.: A. 364 (2004) 1-10.
[6] C. Han, 한국재료학회지. 25 (2015) 398-402.
[7] R. Braun, C. Leyens, M Frohlich, Mater. Corrosion. 56 (2005) 930-936.
[8] W.J. Zhang, L. Francesconi, E. Evangelista, Mater. Let. 27 (1996) 135-138.
[9] K. Kothari, R. Radhakrishnan, N.M. Wereley, Prog. Aerospace Sci. 55 (2012) 1-16.
[10] G. Wnag, M. Dahms, JOM. 45(1993) 52-56.
[11] H.Q. Ye, Mater. Sci. Eng.: A. 263 (1999) 289-295.
[12] V.N. Eremenko, Ya.V. Natanzon, V. Y. Petrishchev, Powder Metall. Met. Ceram. 26 (1987) 118-122.
[13] A. Taotao, Chinese Journal of Aeronautics. 21 (2008) 559-564.
[14] G. Baudana, S. Biamino, D. Ugues, M. Lombardi, P. Fino, M. Pavese, C. Badini, Powder Metall. Report. 71 (3) 193-199.
[15] V.K. Balla, M. Das, A. Mohammad, A.M. Al-Ahmari, Advanced Eng. Mater. 18 (7) (2016) 1208-1215.

[16] I. Shishkovsky, F. Missemer, I. Smurov, Phys. Procedia. 39 (2012) 382-391.
[17] B. Guo, J. Zhou, S. Zhang, H. Zhou, Y. Pu, J. Chen, Appl. Surf. Sci. 253 (2007) 9301-9310.
[18] L. Löber, F.P. Schimansky, U. Kühn, F. Pyczak, J. Mater. Process. Technol. 214 (2014) 1852-1860.
[19] J. Gussone, Y. Hagedorn, H. Gherekhloo, G. Kasperovich, T. Merzouk, J. Hausmann, Intermerallics. 66 (2015) 133-140.
[20] H.P. Qu, H.M. Wang, Mater. Sci. Eng.: A. 466 (2007) 187-194.
[21] H.P. Qu, P. Li, S.Q. Zhang, A. Li, H.M. Wang, Mater. Des. 31 (2010) 2201-2210.
[22] Y. Ma, D. Cuiuri, N. Hoye, H. Li, Z. Pan, Metallurgical and Materials Transactions B: Process Metallurgy and Materials Science 45 (2014) 2299-2303.
[23] M. Doi, T. Koyama, T. Taniguchi, S. Naito, Mater. Eng.: A. 329-331 (2002) 227-236.
[24] C. Lei, Q. Xu, Y. Sun, Mater. Sci. Eng:A. 313 (2001) 227-236.
[25] R. Miida, S. Hashimoto, D. Watanabe, Japanese J. Appl. Phys. 21 (1982), L59-L61.
[26] H. Sina, S. Iyengar, J. Thermal Analy. Calorimetry 122 (2015) 689-698.
[27] I.A. Mwamba, L.A. Cornish, E. Van der Lingen, SAIMM 7A (2012) 517-526.
[28] Y. Sun, Y. Zhao, D. Zhang, C. Liu, H. Diao, C. Ma, Transactions of Nonferrous Metals Society of China 21 (2011) 1722-1727.